Synthesis, Biological Evaluation, and Molecular Modeling of Natural and Unnatural Flavonoidal Alkaloids, Inhibitors of Kinases

ARTICLE *in* JOURNAL OF MEDICINAL CHEMISTRY · MARCH 2012

Impact Factor: 5.45 · DOI: 10.1021/jm201727w · Source: PubMed

8 AUTHORS, INCLUDING:

Binh Thanh Nguyen
French National Centre for Scientific Research
51 PUBLICATIONS **512** CITATIONS
SEE PROFILE

Bogdan I. Iorga
Natural Product Chemistry Institute
63 PUBLICATIONS **650** CITATIONS
SEE PROFILE

Laurent Meijer
ManRos Therapeutics
418 PUBLICATIONS **21,108** CITATIONS
SEE PROFILE

Françoise Guéritte
French National Centre for Scientific Research
222 PUBLICATIONS **5,015** CITATIONS
SEE PROFILE

Journal of Medicinal Chemistry

Article

pubs.acs.org/jmc

Synthesis, Biological Evaluation, and Molecular Modeling of Natural and Unnatural Flavonoidal Alkaloids, Inhibitors of Kinases

Thanh Binh Nguyen,[†] Olivier Lozach,[‡] Georgiana Surpateanu,[†] Qian Wang,[§] Pascal Retailleau,[†] Bogdan I. Iorga,[†] Laurent Meijer,*[,∥,‡] and Françoise Guéritte*[,†]

[†]Centre de Recherche de Gif, Institut de Chimie des Substances Naturelles (ICSN), CNRS, 91198 Gif-sur-Yvette Cedex, France

[‡]"Protein Phosphorylation & Human Disease", CNRS, Station Biologique, Place G. Teissier, 29682 Roscoff Cedex, France

[§]Institute of Chemical Sciences and Engineering, Ecole Polytechnique Fédérale de Lausanne, EPFL-SB-ISIC-LSPN, 1015 Lausanne, Switzerland

[∥]ManRos Therapeutics, Centre de Perharidy, 29680 Roscoff, France

Supporting Information

ABSTRACT: The screening of the ICSN chemical library on various disease-relevant protein kinases led to the identification of natural flavonoidal alkaloids of unknown configuration as potent inhibitors of the CDK1 and CDK5 kinases. We thus developed an efficient and modular synthetic strategy for their preparation and that of analogues in order to determine the absolute configuration of the active natural flavonoidal alkaloids and to provide further insights on the structure–activity relationships in this series. The structural determinants of the interaction between some flavonoidal alkaloids with specific kinases were also evaluated using molecular modeling.

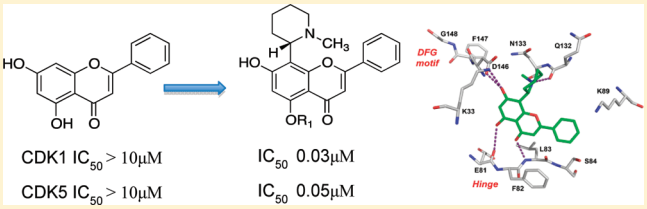

1. INTRODUCTION

Cyclin-dependent kinases (CDKs),[1] glycogen synthase kinase-3 (GSK3),[2] dual specificity tyrosine-phosphorylation-regulated kinase 1A (DYRK1A),[3] and cdc2-like kinase CLK1[4] are serine–threonine kinases that attract considerable interest because of their involvement in many essential physiological processes and multiple human diseases such as cancer and neurodegenerative diseases.[1] Today, around 250 small molecule kinase inhibitors are undergoing clinical trials for the treatment of cancer and other diseases, showing that kinases constitute important therapeutic targets. Our interest in the synthesis of kinase inhibitors comes from the screening of the ICSN–CNRS chemical library, comprising about 4000 natural and synthetic products. The screening on five kinases, CDK1, CDK5, GSK3, CLK1, and DYRK1A, led to the selection of two natural flavonoidal alkaloids which possess a good inhibitory activity on the cyclin-dependent kinases CDK1/cyclin B and CDK5/p25 by ATP competition: *O*-demethylbuchenavianine (**1**)[5,6] and *N*,*O*-didemethylbuchenavianine (**2**)[5,6] (Figure 1) found in the fruits of *Buchenavia macrophylla* and in the leaves of *Buchenavia capitata*.

Capitavine (**3**),[5] isolated from the seeds of *B. capitata*, *N*-demethylbuchenavianine (**4**),[5] and buchenavianine (**5**)[5,6] as well as chrysin (**6**)[7] (Figure 1), also present in the ICSN chemical library, were found less active on the five kinases (IC_{50} > 10 μM) (Table 1). These preliminary results showed that (1) the 8-substituted regioisomer **1** was more active than its 6-substituted analogue **3** and (2) the amino moiety and the free hydroxyl group at C-5 of flavonoidal alkaloids were essential for interaction with these kinases. It should be noted that the flavonoidal alkaloids **1**–**5** were optically active, but their absolute configuration was unknown at this time. The structure of these molecules is reminiscent of flavopiridol (**7**), the first synthetic cCDK inhibitor to enter clinical trials as an anticancer drug.[8] Similar to flavopiridol, a new synthetic flavonoidal alkaloid (P276–00) **8** enters clinical studies as a small-molecule CDK inhibitor[9] (Figure 1). Since the discovery of the

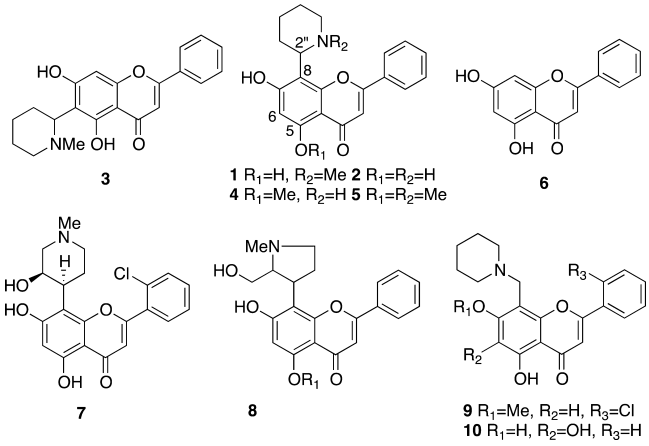

Figure 1. Natural flavonoids (**1**–**6**) and synthetic flavonoidal alkaloids (**7**–**10**).

Received: December 22, 2011
Published: February 21, 2012

Table 1. Synthesis of 6- and 8-Substituted Flavonoidal Alkaloids from 6

entry	conditions	6-sub/8-sub	yield (%)
1a	40 °C, H_2O/THF	100/0	95 (**13**)
1b	110 °C, H_2O/THF	5/1	nd (**13**)/nd (**16**)
2a	40 °C, H_2O	100/0	80 (**12**)
2b	80 °C, H_2O/THF	5/1	13 (**12**)/7 (**15**)
3a	40 °C, H_2O/THF	100/0	87 (**14**)
3b	120 °C, H_2O/THF	5/1	11 (**2**)/nd (**14**)
4a	40 °C, H_2O/THF	100/0	78 (**3**)
4b	110 °C, H_2O/THF	24/1	nd (**3**)/ nd (**1**)

antitumor activity of flavopiridol, studies concerning the structure–activity relationships have been realized on nitrogen-containing flavonoids active on kinases. For example, the piperidinylmethyl analogues of flavopiridol **9**[10] as well as that of baicalein **10**[11] (Figure 1) are good inhibitors of CDK1/cyclin B. These studies have shown that the position of the piperidine ring as well as the position of the atom nitrogen play critical role in the kinase inhibitory activity.

In the present study, we report the synthesis of natural and non-natural flavonoidal alkaloids as well as the absolute configuration of the active natural flavonoidal alkaloids. We also provide further insights on the structure–activity relationships in this series as well as the structural determinants of the interaction between these flavonoids with specific kinases identified using molecular modeling.

2. SYNTHESIS AND KINASE INHIBITORY ACTIVITY

2.1. Synthesis of 6- and 8-Substituted Flavonoidal Alkaloids. Modifications were carried out by varying the substitution position of the alkaloid moiety, the ring size, ring vs open chain structure, and alkylation degree of the nitrogen atom. We recently reported the phenolic Mannich reaction between **6** and the bench-stable iminic compound **11a** or iminium precursor **11b** as a method of choice for a one-step, straightforward access to the 6-substituted **3**,[5] **14**,[5] **12**,[12,13] and **13** or 8-substituted **16**[12,13] and **2**[5,6] flavonoidal alkaloids (Scheme 1).[14] We also describe here the synthesis of ficine

Scheme 1. Synthetic Route to compounds 1–3 and 12–16[14]

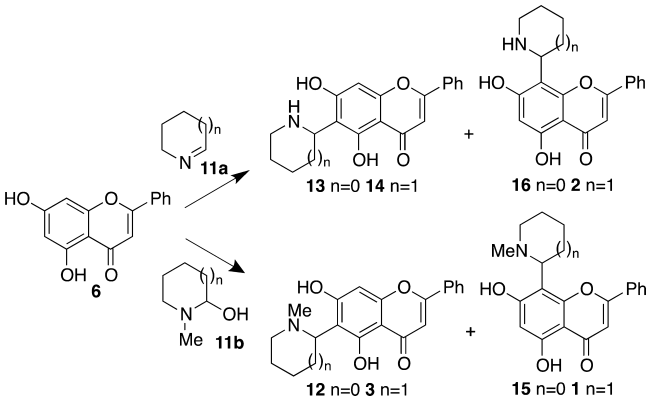

15 and isoficine **12** under the same conditions. Thus, the reaction performed in aqueous medium at 40 °C, in the mixture of H_2O–THF, was highly regioselective and afforded the 6-substituted adduct as major or unique product in excellent yields for all iminic starting materials (Scheme 1 and Table 1).[14] As shown in Table 1 (entries 1b–4b), the yield of 8-substituted adduct increased when the reaction was performed at elevated temperature.

Having an important quantity of **3** in hand, we were looking for a convenient alternative approach to its 8-substituted regioisomer **1**. The Wessely–Moser rearrangement[15] has been known as an important method in structure elucidation and synthesis of flavonoids, involving the interconversion between 8- and 6-substituted flavone under acidic conditions.[16] Thus, heating neat triflate salt of capitavin at 180 °C afforded cleanly a mixture of both regioisomers (6-sub/8-sub = 3:1) without noticeable degradation. In that way, compound **1** was obtained from capitavin with a 22% yield. We then prepared adducts derived from chrysin, hexanal, and methylamine (Scheme 2). The 6-substituted aminoalkylflavone **17** was obtained predominantly (78%) when **6** was reacted with hexanal (2 equiv) and methylamine (6 equiv). When methylamine was used in excess (20 equiv), the ratio of **17** to the 8-substituted regioisomer **18** decreases to 2:1 (Scheme 2). In all cases, both regioisomers could be separated efficiently by flash column chromatography on silica gel.

We focused next our efforts on the enantiomeric separation of the three most active racemic 8-substituted adducts: **1**, **15**, and **18**. These separations, which were realized by SFC HPLC using IC column, afforded the desired enantiomers in satisfactory enantiomerical purities. Absolute configuration of a single enantiomer was determined unambiguously by X-ray crystallography. Thus, (+)-**1** and (+)-**15** have the (*R*)-configuration, whereas (−)-**18** was (*S*) (see Supporting Information). Natural **1** has a negative optical rotation ($[\alpha]_D^{23}$ −21 (*c*, 0.13, $CHCl_3$), and its HPLC analysis shows an *ee* of 20% enriched in (*S*) isomer (more retained). We thus assumed that during the isolation process, which was carried out in highly basic conditions (aqueous ammonia solution), partial racemization occurred.

2.2. Biological Evaluation of Flavonoidal Alkaloids. The compounds were evaluated for their potential inhibitory effects on purified kinases (CDK1, CDK5, GSK3, CLK1, and DYRK1A) as described in the Experimental Section. The 6-substituted flavones **3**, **12**, **13**, **14**, and **17** were found to much more less active ($IC_{50} \gg 10$ μM) than their 8-substituted regioisomers **1**, **15**, **16**, **2**, and **18**, respectively. Thus, Table 2 summarizes the biological evaluation on the five kinases of the 8-substituted isomers together with that of each enantiomers of **1**, ficine **15**, and **18**. The IC_{50} values were determined from dose–response curves and compared to those of the reference molecule, flavopiridol.

Like for flavopiridol, the cyclin-dependent kinases CDK1 and CDK5 are more sensitive to the flavonoidal alkaloids than GSK3 and CLK1. One important point is that the *N*-methylation of the amino moiety is essential for a better interaction with kinases. Indeed, **1** and **15** are 50 and 30 times more active on CDK1 than their *N*-demethylated analogues **2** and **16**, and more active also on the other kinases CDK5, GSK3, and CLK1. Additionally, a free hydroxyl group at the C-5 position is essential for a good interaction with kinases because the IC_{50} of **5** was superior to 10 μM. These observations are in full agreement with the interactions revealed by molecular docking calculations (see below). It should be noted that **1** and **15** have a CDK1/cyclin B inhibitory activity similar to that of bacalein analogues containing a nitrogen ring at C-8 and a free hydroxyl group at C-7, such as **10**.[11] Thanks to the separation of each enantiomer of the racemic mixtures of **1** and **15** and X-ray analysis of one of the enantiomers, we

dx.doi.org/10.1021/jm201727w | J. Med. Chem. 2012, 55, 2811–2819

Scheme 2. Synthesis of 6- and 8-Substituted Aminoalkylflavones[a]

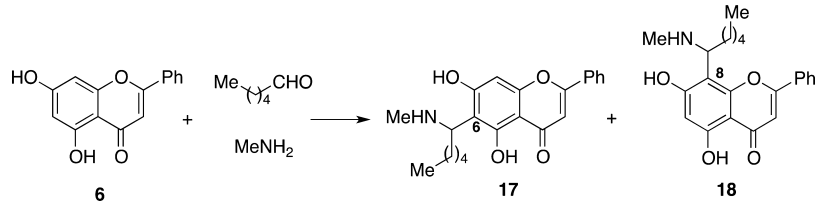

[a]Reaction conditions: H_2O−THF, 40 °C, 5 h

Table 2. Kinases Activity of 8-Substituted Flavonoidal Alkaloids

	kinases inhibitory activities (IC_{50} in μM)				
compd	CDK1	CDK5	GSK3	CLK1	DYRK1A
1	0.09	1.7	5.1	8.5	>10
(*R*)-(+)-**1**	1.1	0.95	≥10	>10	>10
(*S*)-(−)-**1**	0.03	0.05	1.6	2.1	>10
(±)-**2**	5	5.5	>10	>10	>10
4	>10	>10	>10	>10	>10
5	>10	>10	>10	>10	>10
(±)-**15**	0.05	0.09	1.3	1.6	>10
(*R*)-(+)-**15**	0.39	0.57	2.6	7.4	>10
(*S*)-(−)-**15**	0.04	0.04	0.72	0.67	>10
(±)-**16**	1.6	1.1	>10	>10	>10
(±)-**18**	1.1	0.52	5.2	>10	>10
(*R*)-(+)-**18**	0.52	0.27	4.1	>10	>10
(*S*)-(−)-**18**	5.4	2.1	>10	>10	>10
7	0.09	0.06	0.36	1.3	0.3

could assign the *S* configuration to the most active enantiomers of **1** and **15**. If racemic **1** and ficine **15** turned out to inhibit CDK1 and CDK5 as potently as flavopiridol, their (*S*)-enantiomer was slightly more active than flavopiridol, inhibiting CDK1 and CDK5 with IC_{50} value around 0.04 μM. These flavonoidal alkaloids were generally less active on the GSK3 and CLK1 kinases. Only (*S*)-**1** retains a good activity, with an IC_{50} similar to that of flavopiridol on these two kinases. Moreover, the flavonoidal alkaloids are inactive toward DYRK1A at 10 μM, while flavopiridol, the reference compound, showed a micromolar inhibition of this enzyme. Compound **18** with an opened amino side chain at C-8 is also less active than compounds **1** and **15** possessing a nitrogen-containing heterocycle at that position. After separation of the racemic mixture **18** and X-ray analysis of one of the enantiomers, we could assign the (*R*) configuration to the most active enantiomer, which is contradictory to the results obtained for ficine and (*O*)-demethylbuchenavianine.

To better understand the interaction pattern at the molecular level between the flavonoidal alkaloids and these kinases, molecular modeling calculations were carried out and the results compared with the experimental data.

3. MOLECULAR MODELING

Three-dimensional crystal structures are available in the Protein Data Bank (PDB)[17] for four proteins included in this study: CDK5 (entry 1UNL),[18] GSK3 (entry 1J1B),[19] CLK1 (entry 1Z57), and DYRK1A (entry 2VX3). As no structure was available for CDK1, a homology model was built using the DFG-in structure of CDK2 (entry 1YKR,[20] sharing 65% sequence identity with CDK1) as template and the sequence alignment presented in Figure S2 of the Supporting Information). These structures present well conserved geometries, with backbone root-mean-square deviations (rmsd) of 2.05, 2.33, 1.98, and 2.63 Å for GSK3, CLK1, DYRK1A, and CDK1, respectively, compared with CDK5.

The overall sequence identity between these kinases sequences ranges from 32% to 57%, with values of 30−76% for the binding site region (defined as a sphere with a 6.0 Å radius around the aspartate residue from the DFG motif). A notable exception is DYRK1A, which shows sensibly lower values, 12−15% and 31−34%, respectively. Selected residues from the ATP binding site presenting amino acid variability are shown in Table S1 of the Supporting Information). Some of these residues play an important role in the ligand selectivity determined experimentally.

From the ligand side, the crystal structure of a synthetic flavonoid analogue, flavopiridol (**7**, Figure 1), in complex with CDK9/CycT1 (PDB entry 3BLR), was recently reported.[21] This ligand binds to the ATP-binding pocket of CDK9 and has a remarkable structural similarity with the compounds studied in this work. The overall sequence identity of CDK9 with CDK1, CDK5 and GSK3 is about 40−46% and only 22% with CLK1, whereas for the binding site region it increases to 53−68% and 30%, respectively. Therefore, all docking results obtained in this study were critically compared with the flavopiridol/CDK9 complex, which can be considered as representative for the interaction of kinases with flavonoid compounds.

The docking procedure was first evaluated by the direct docking of flavopiridol into the native CDK9 structure and by cross-docking with the other kinase structures included in this study. The protein−ligand complex was correctly reproduced in direct docking (rmsd 0.6 Å) and the cross-docking provided similar conformations, thus validating the procedure that will be further used for the docking of new compounds (Table 2 and Figure S3 in the Supporting Information). In the following paragraphs, only the interactions between the active compounds (**1**, **2**, **15**, **16**, **18**) and the corresponding proteins are discussed. The inactive compounds generally show unspecific binding modes inside or outside the ATP binding pocket. A particular example is DYRK1A, for which docking calculations could evidence no specific interactions with any of the ligands included in this work, in agreement with the experimental data. However, **7** is a notable exception to this rule, being the only member of this class of compounds showing a biological activity against DYRK1A. A possible explanation for this behavior is the presence of a Val172 residue in DYRK1A just before the DFG motif, whereas in the equivalent positions of CDK1 and CDK5, the smaller residues Ala145 and Ala143 are present, respectively. As a consequence, in the latter case this region of the binding site can accommodate the substituents (e.g., NMe in **1** or **15**) surrounding the protonated amino group, while the Val172 would induce steric clashes with these

dx.doi.org/10.1021/jm201727w | J. Med. Chem. 2012, 55, 2811−2819

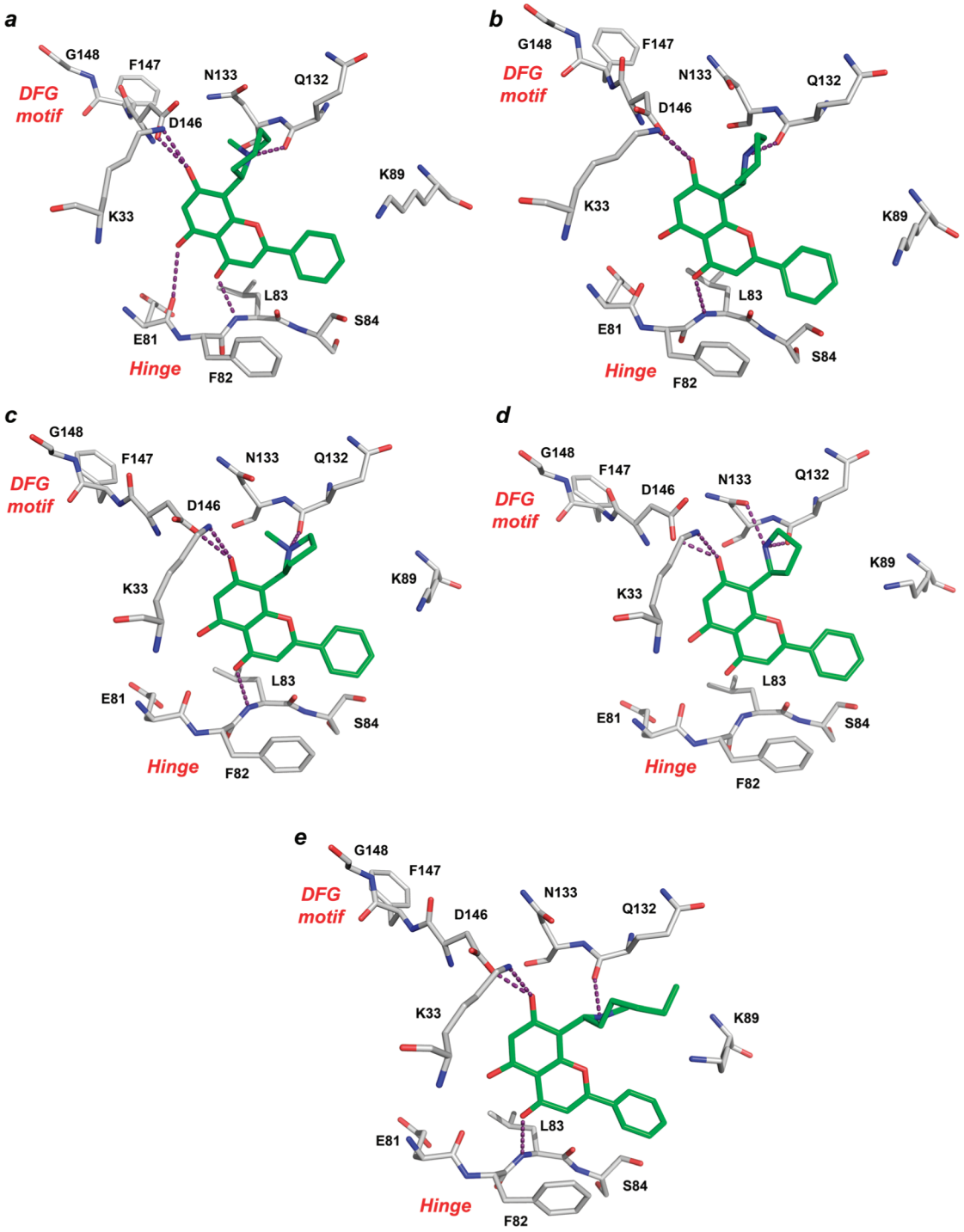

Figure 2. Docking poses for complexes of CDK1 with compounds **1** (a), **2** (b), **15** (c), **16** (d), and **18** (e).

substituents, which can explain the absence of biological activity observed experimentally for the compounds included in this study against DYRK1A (Table 2). On the contrary, **7** has the NMe group in a different position on the ring and thus the clashes with Val172 are absent.

3.1. Docking with CDK1 and CDK5. Compounds **1**, **2**, **15**, **16**, and **18** were identified to interact favorably with the CDK1 and CDK5 binding sites (Figures 2 and 3). These two binding sites are very similar, the only differences being Leu83/Cys83 and Ser84/Asp84 in CDK1/CDK5, respectively. The mutation D144N in the CDK5 crystallographic structure should also be noted. However, all these differences do not influence the main binding pattern and these five compounds (**1**, **2**, **15**, **16**, and **18**) interact in a similar manner with CDK1 and CDK5. The phenyl substituent points out toward the outside of the binding pocket, and the flavone ring system establishes hydrogen bonds with the NH backbone group of Leu83/Cys83 via the chromone oxygen and with Asp146/Asn144 via the C-7 hydroxyl group. In CDK1, this hydroxyl group also interacts with the side chain of Lys33. Another conserved feature in this system is the interaction between the protonated amino group of the ligand with the backbone carbonyl group of Gln132/

dx.doi.org/10.1021/jm201727w | J. Med. Chem. 2012, 55, 2811−2819

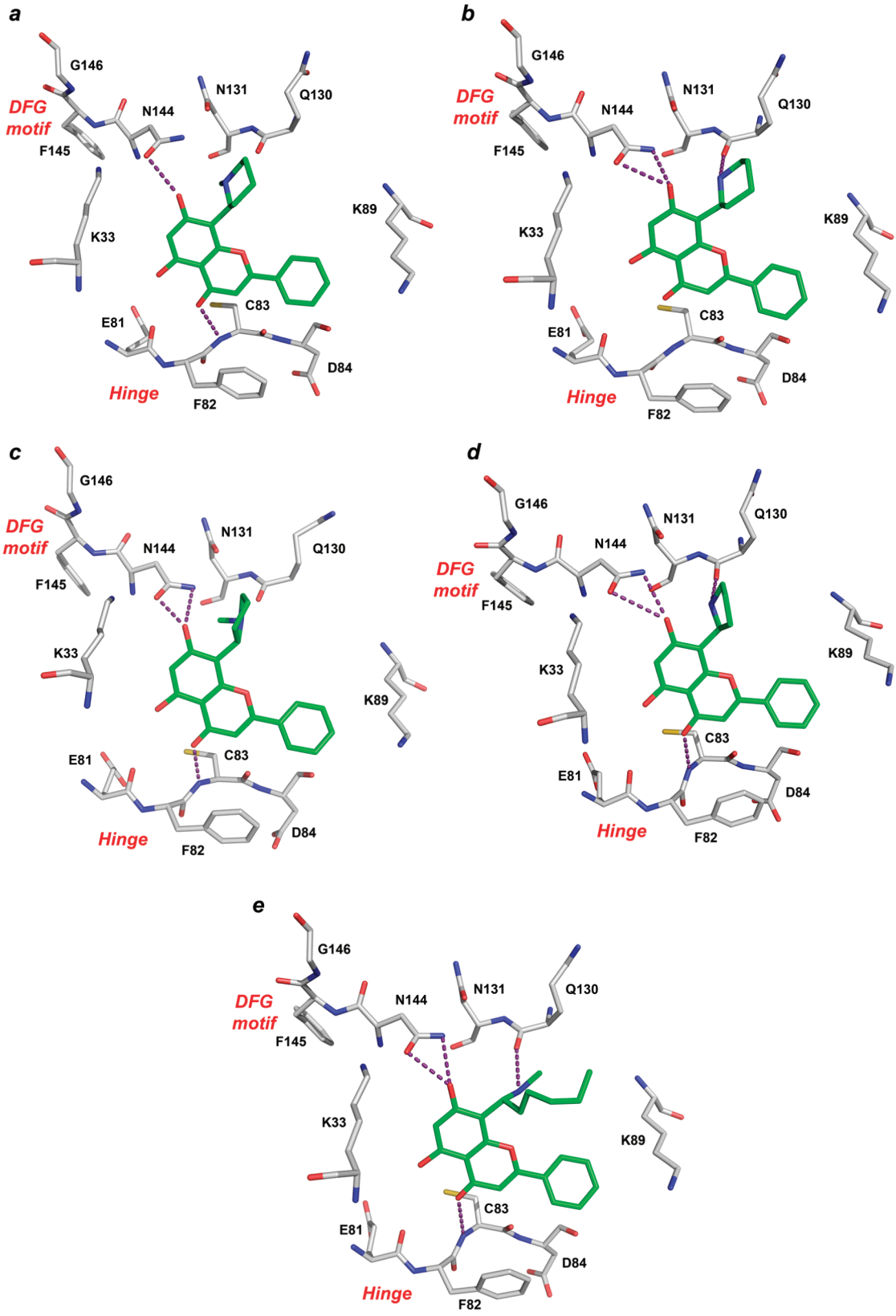

Figure 3. Docking poses for complexes of CDK5 with compounds **1** (a), **2** (b), **15** (c), **16** (d), and **18** (e).

Gln130. Both configurations were considered in the docking process. For compound **18**, the isomer with *R* configuration was found to establish better interactions with the active site residues, whereas for compounds **1**, **2**, **15**, and **16**, the *S* isomer was predicted to be more potent. These results are in agreement with the biological activities and X-ray diffraction data (Table 2).

3.2. Docking with GSK3. Molecular docking calculations showed that GSK3 is able to interact favorably only with compounds **1**, **15**, and **18**. The binding modes are generally

dx.doi.org/10.1021/jm201727w | *J. Med. Chem.* 2012, 55, 2811−2819

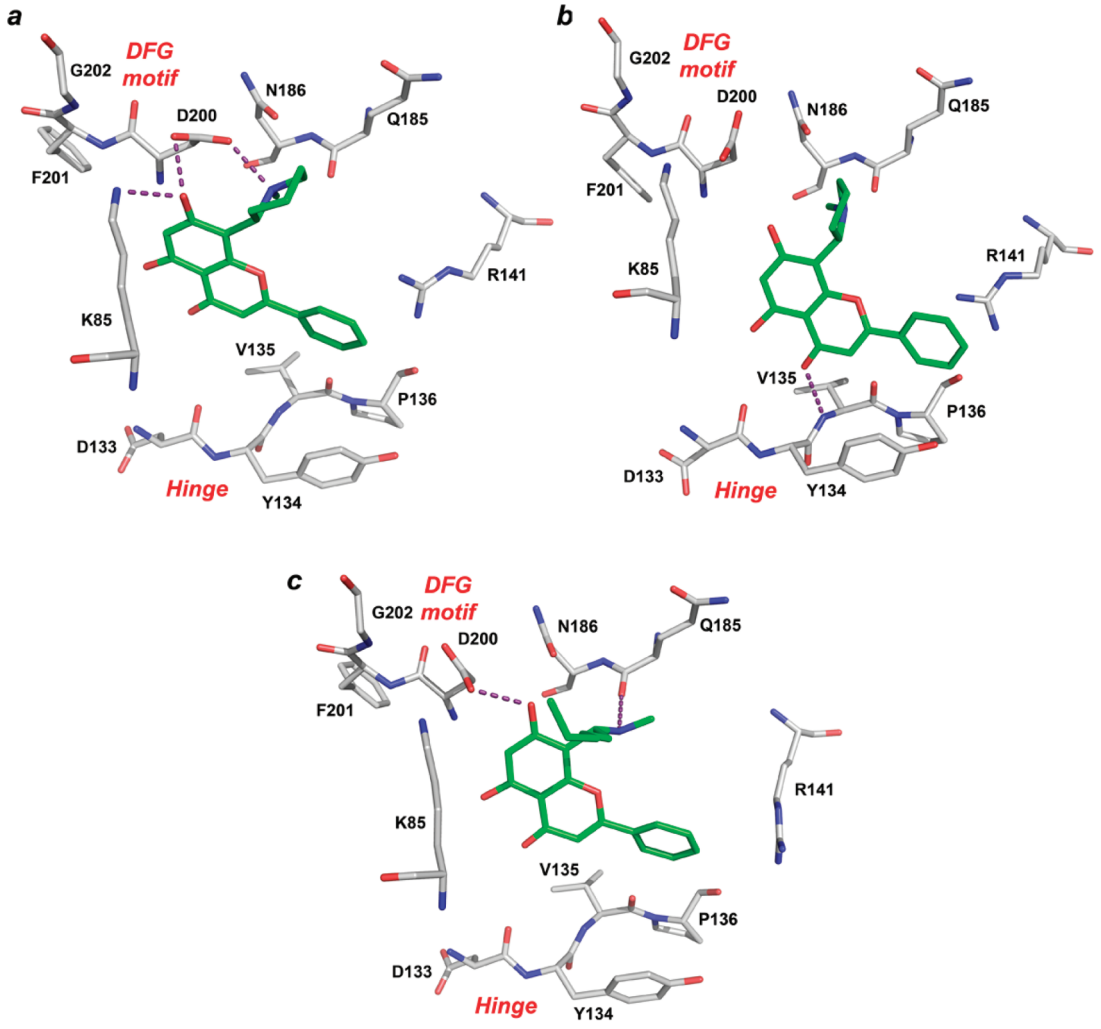

Figure 4. Docking poses for complexes of GSK3 with compounds **1** (a), **15** (b), and **18** (c).

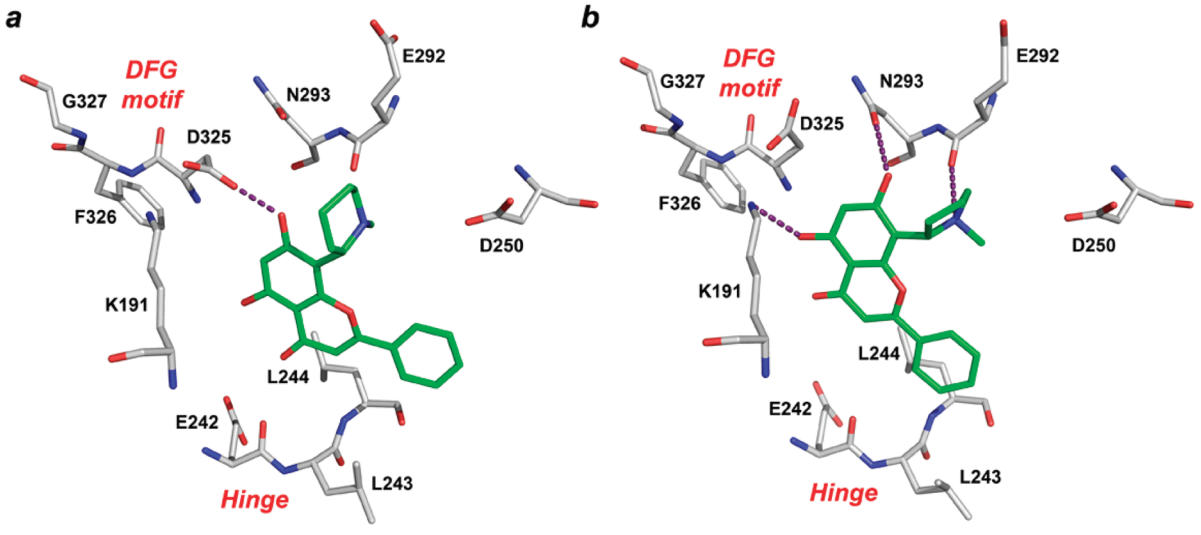

Figure 5. Docking poses for complexes of CLK1 with compounds **1** (a) and **15** (b).

similar with those evidenced in the case of CDK1 and CDK5, with the phenyl substituent pointing out toward the outside of the active site, but with the notable difference that the ligand is buried more deeply into the ATP binding pocket. This is mainly due to the presence of Arg 141 (instead of Lys in CDK1 and CDK5, smaller and more flexible) and to a different conformation of the loop Val 61−Tyr 71 in GSK3. The consequence of these changes in the binding site conformation is that the ligands (compounds **1**, **15**, and **18**) do not have anymore optimal interactions with neighboring residues and

dx.doi.org/10.1021/jm201727w | *J. Med. Chem.* 2012, 55, 2811−2819

only a limited number of hydrogen bonds is observed either with the DFG or the hinge residues (Figure 4). Again, the *R* isomer is predicted to be more active for compound **18** and the *S* isomer in the case of compounds **1** and **15**. These results are also in agreement with the kinase activity (Table 2).

3.3. Docking with CLK1. Compared with the previous three proteins, CLK1 presents similar features within the binding pocket. However, the solvent-exposed surface is slightly different, which is mainly due to a conformation of the loop Thr 166−Val 176 similar to those observed for GSK3, and to the presence of Asp 250 (instead of Arg or Lys) and Leu 243 (instead of Phe or Tyr). These changes in the active site conformations allow the interaction with only a few ligands (compounds **1** and **15**) and only through the DFG loop of the binding pocket (Figure 5). The general orientation of the ligand is similar to the one observed previously, with the phenyl substituent toward the outside of the binding pocket. Additionally, the *S* isomer of compounds **1** and **15** was predicted to establish more favorable interactions with the active site residues than the R isomer. Again, this is in line with the activity of flavonoids **1**−**18** found for kinase CLK1 (Table 2).

4. CONCLUSION

The screening of the ICSN−CNRS chemical library has resulted in the selection of two natural flavonoidal alkaloids, **1** and **2**, which possess a good inhibitory activity on the cyclin-dependent kinases CDK1/cyclin B and CDK5/p25. The results of this screening showed also that the substitution of chrysin by piperidine or pyrrolidine was to be located at C-8 and not C-6 to get active flavonoidal alkaloids. This led us to develop syntheses for an easy access to racemic natural and unnatural flavonoidal alkaloids, in order to gain more insight into the structure−activity relationships in this series. Thank to SFC chromatography and X-ray crystallography, each enantiomer of the three racemic mixtures could be separated for biological evaluation. Thus, it was shown that **1** and **15** bearing a piperidine and pyrrolidine ring, respectively, were most active on kinases CDK1, CDK5, GSK3, and CLK1, in their *S*-configuration. On the contrary, the most active enantiomer, **18**, with an opened amino side chain, has the *R* configuration. If **1** and **18** displayed potent inhibition of CDK1 and CDK5, they are less active on GSK3 and CLK1 and inactive on DYRK1A at 10 μM. Only **15** is as active as flavopiridol on the four kinases CDK1, CDK5, GSK3, and CLK1 but inactive on DYRK1A at 10 μM. The differences in activity of these flavonoidal alkaloids could be explained by molecular docking studies of each enantiomer at the active site of each kinase.

5. EXPERIMENTAL SECTION

5.1. Kinase Preparations and Assays. Kinase activities were assayed in buffer A (10 mM $MgCl_2$, 1 mM EGTA, 1 mM DTT, 25 mM Tris-HCl pH 7.5, 50 μg heparin/mL, supplemented extemporaneously with 0.15 mg BSA/mL), at 30 °C, at a final ATP concentration of 15 μM. Blank values were subtracted and activities expressed in % of the maximal activity, i.e., in the absence of inhibitors. Controls experiments were performed with appropriate dilutions of DMSO.

CDK1/cyclin B (M phase starfish oocytes, native) and CDK5/p25 (human, recombinant) were prepared as previously described.[22] Their kinase activity was assayed in buffer A, with 25 μg of histone H1, in the presence of 15 μM [γ-^{33}P] ATP (3,000 Ci/mmol; 10 mCi/ml) in a final volume of 30 μL. After 30 min incubation at 30 °C, the reaction was stopped by harvesting onto P81 phosphocellulose papers (Whatman) using a FilterMate harvester (Packard), and papers were washed in 1% phosphoric acid. Scintillation fluid was added and the radioactivity measured in a Packard counter.

GSK-3α/β (porcine brain, native) was purified (Primot et al., 2000)[23] and assayed, as described for CDK1 but using a GSK-3 specific substrate (GS-1: YRRAAVPPSPSLSRHSSPHQSpEDEEE) (pS stands for phosphorylated serine), synthesized by Proteogenix (Oberhausbergen, France).

DYRK1A (rat, recombinant, expressed in *Escherichia coli* as a GST fusion protein) was purified by affinity chromatography on glutathione−agarose and assayed as described for CDK1/cyclin B using Woodtide (KKISGRLSPIMTEQ) (1 μg/assay) as a substrate.

CLK1 (mouse, recombinant, expressed in *E. coli* as GST fusion proteins) was assayed in buffer A with RS peptide (GRSRSRSRSRSR) (1 μg/assay).

5.2. Chemistry. Reagents were obtained from commercial suppliers and used without further purification unless otherwise noted. Analytical thin layer chromatography (TLC) was purchased from Merck KGaA (silica gel 60 F_{254}). Visualization of the chromatogram was performed by UV light (254 nm) or phosphomolybdic acid and vanilline stains. Flash column chromatography was carried out using Kieselgel 35−70 μm particle sized silica gel (230−400 mesh).

^{1}H chemical shifts are reported in ppm (δ) relative to tetramethylsilane (TMS) with the solvent resonance employed as the internal standard ($CDCl_3$, δ 7.24 ppm). Data are reported as follows: chemical shift, multiplicity (s = singlet, d = doublet, t = triplet, q = quartet, m = multiplet), coupling constants (Hz), and integration. ^{13}C chemical shifts are reported in ppm (δ) from TMS, with the solvent resonance as the internal standard ($CDCl_3$, δ 77.0 ppm).

Mass spectra were determined on an AEI MS-9 using electron spray ionization (ESI). Piperideine[24] and pyrroline[25] were synthesized by the known methods. Compounds **2**, **3**, and **12**−**14** were prepared according to the procedure published by our group.[14]

Analytical and preparative high performance liquid chromatography (HPLC) was performed on TharSFC superchrom equipped with diode array UV detectors, using IC (4.6 mm × 250 mm) column. Optical rotation measurement was performed on a MCP 300/500 Anton Paar digital polarimeter.

CCDC 846440 (**1**), CCDC 846439 (**15**), and CCDC 846441 (compound **18**) contain the supplementary crystallographic data for this paper. These data can be obtained free of charge from The Cambridge Crystallographic Data Centre via www.ccdc.cam.ac.uk/data_request/cif.

5,7-Dihydroxy-8-(1-methylpiperidin-2-yl)-2-phenyl-4H-chromen-4-one ((±)-1). Triflic acid (250 μL, 426 mg, 2.84 mmol) was added dropwise to a solution of **3** (1.00 g, 2.84 mmol) in CH_2Cl_2 (4 mL) at 0 °C. The resulting solution was concentrated in vacuo. The yellow salt was then heated under agon at 180 °C for 16 h. The reaction mixture cooled to rt was treated cautiously with a saturated aqueous solution of $NaHCO_3$ (5 mL) and AcOEt (20 mL) with vigorous stirring. The separated aqueous layer was extracted with AcOEt (2 × 10 mL). The combined organic layers were dried (Na_2SO_4) and concentrated. The residue (**1**/**3** = 1:3 by ^{1}H NMR) was purified by flash column chromatography (AcOEt/MeOH 10:0 to 95:5) to afford F1 (±)-**1** (217 mg, 22%) and F2 **3** (652 mg, 65%) as yellow crystals. Data for (±)-**1**: ^{1}H NMR (300 MHz, $CDCl_3$) δ 13.10 (s, 1H), 7.87−7.84 (m, 2H), 7.51−7.46 (m, 3H), 6.60 (s, 1H), 6.46 (s, 1H), 3.80 (dd, J = 11.4, 3.7 Hz, 1H), 3.24−3.16 (m, 1H), 2.30 (s, 3H), 2.30−2.11 (m, 1H), 1.95−1.61 (m, 5H), 1.49−1.33 (m, 1H). ^{13}C NMR (75 MHz, $CDCl_3$) δ 182.6, 165.5, 163.7, 158.5, 157.3, 131.8, 129.2, 126.4, 110.3, 105.7, 104.4, 100.6, 94.9, 61.1, 55.0, 43.8, 30.9, 25.6, 23.9. HRMS: m/z [M + H]$^+$ calcd for $C_{21}H_{22}NO_4$, 352.1549; found, 352.1550. F1 was next subjected to SFC HPLC separation using, column IC, 30% cosolvents (iPrOH/MeOH/diethylamine 50:50:1), flow rate 4 mL/min; t_{R1} = 10.1 min, 96 mg, *ee* > 99%, $[\alpha]_D^{23}$ +122 (*c*, 0.1, $CHCl_3$), configuration *R* (determined by X-ray diffraction); t_{R2} = 17.7 min (102 mg, *ee* = 96%, $[\alpha]_D^{23}$ −104 (*c*, 0.1, $CHCl_3$) configuration *S*. Natural product **1** has a negative optical rotation ($[\alpha]_D^{23}$ −21 (*c*, 0.13, $CHCl_3$), and its HPLC analysis shows an *ee* of 20% enriched in (*S*) isomer (more retained).

*5,7-Dihydroxy-8-(1-methylpyrrolidin-2-yl)-2-phenyl-4H-chromen-4-one ((±)-**15**).* A mixture of chrysin (2.03 g, 8 mmol) and freshly prepared 2-hydroxy-1-methylpyrrolidine (1.21 g, 12 mmol) in water (4 mL) and THF (4 mL) was heated at 80 °C in a sealed tube for 5 h and then cooled to rt and diluted with CH_2Cl_2 (30 mL) and H_2O (10 mL). The mixture was filtered to remove trace of insoluble chrysin. The separated aqueous layer of the filtrate was extracted with CH_2Cl_2 (2 × 10 mL). The combined organic layers were dried (Na_2SO_4) and concentrated. The residue (**15**/**12** = 1:5 by ^{1}H NMR) was purified by flash column chromatography (AcOEt/MeOH 10:0 to 95:5) to afford F1 (±)-**15** (347 mg, 13%) and F2 (**12**) (1923 mg, 71%) as yellow crystals. Data for (±)-**15**: ^{1}H NMR (300 MHz, $CDCl_3$) δ 12.65 (s, 1H), 7.81−7.78 (m, 2H), 7.54−7.24 (m, 3H), 6.62 (s, 1H), 6.26 (s, 1H), 4.13 (t, J = 8.5 Hz, 1H), 3.41−3.34 (m, 1H), 2.56−2.37 (m, 2H), 2.43 (s, 3H), 2.05−1.86 (m, 3H). ^{13}C NMR (75 MHz, $CDCl_3$) δ 182.5, 166.0, 163.1, 161.5, 155.1, 132.0, 131.9, 129.4, 126.2, 106.1, 104.7, 102.6, 100.9, 64.7, 55.7, 40.7, 32.9, 23.4. HRMS: m/z $[M + H]^+$ calcd for $C_{20}H_{20}NO_4$, 338.1392; found, 338.1381. Then 200 mg of F1 was next subjected to SFC HPLC separation using column IC, 50% cosolvents (iPrOH/diethylamine 99:1), flow rate 4 mL/min; t_{R1} = 5.8 min, 78 mg, *ee* > 99%, $[\alpha]_D^{23}$ −160 (*c*, 0.1, $CHCl_3$), configuration *S*; t_{R2} = 6.9 min, 85 mg, *ee* = 92%, $[\alpha]_D^{23}$ +144.5 (*c*, 0.11, $CHCl_3$), configuration *R* (determined by X-ray diffraction).

*5,7-Dihydroxy-8-(1-(methylamino)hexyl)-2-phenyl-4H-chromen-4-one ((±)-**18**) and 5,7-Dihydroxy-6-(1-(methylamino)hexyl)-2-phenyl-4H-chromen-4-one ((±)-**17**).* A mixture of chrysin (2.03 g, 8 mmol) and hexanal (1.00 g, 10 mmol) in an aqueous solution $MeNH_2$ (40% in water, 6.2 g, 80 mmol) was heated in a sealed tube at 40 °C for 5 h and then cooled to rt and diluted with CH_2Cl_2 (30 mL) and H_2O (10 mL). The mixture was filtered to remove trace of insoluble chrysin. The separated aqueous layer of the filtrate was extracted with CH_2Cl_2 (2 × 10 mL). The combined organic layers were dried (Na_2SO_4) and concentrated. The residue (8-substituted: 6-substituted = 1:2 by ^{1}H NMR) was purified by flash column chromatography (AcOEt/MeOH 10:0 to 95:5) to afford F1 5,7-dihydroxy-8-(1-(methylamino)hexyl)-2-phenyl-4*H*-chromen-4-one (793 mg, 27%) and F2 5,7-dihydroxy-6-(1-(methylamino)hexyl)-2-phenyl-4*H*-chromen-4-one (2.42 g, 67%) as yellow crystals. Under other conditions in which a mixture of chrysin (254 mg, 1 mmol), hexanal (200 mg, 2 mmol), and $MeNH_2$ (40% in water, 0.46 mL, 6 mmol) was heated in a sealed tube at 40 °C for 16 h then cooled to rt and subjected to the same treatment, 5,7-dihydroxy-6-(1-(methylamino)hexyl)-2-phenyl-4*H*-chromen-4-one was obtained preponderantly (286 mg, 78%). (±)-**18**: ^{1}H NMR (300 MHz, $CDCl_3$) δ 12.72 (s, 1H), 7.82−7.80 (m, 2H), 7.54−7.24 (m, 3H), 6.63 (s, 1H), 6.25 (s, 1H), 4.38 (t, J = 6.8 Hz, 1H), 2.47 (s, 3H), 1.87−1.79 (m, 2H), 1.49−1.16 (m, 6H), 0.77 (t, J = 7 Hz, 3H). ^{13}C NMR (75 MHz, $CDCl_3$) δ 182.6, 166.2, 163.1, 161.5, 155.2, 131.9, 129.4, 126.2, 106.0, 104.8, 102.8, 100.9, 59.1, 35.8, 34.6, 31.8, 25.9, 22.7, 14.1. HRMS: m/z $[M + H]^+$ calcd for $C_{22}H_{26}NO_4$, 368.1862; found, 368.1850. (±)-**17**: ^{1}H NMR (300 MHz, $CDCl_3$) δ 13.09 (s, 1H), 7.85−7.81 (m, 2H), 7.48−7.36 (m, 3H), 6.58 (s, 1H), 6.36 (s, 1H), 4.25 (t, J = 6.8 Hz, 1H), 2.44 (s, 3H), 1.83−1.66 (m, 2H), 1.49−1.16 (m, 6H), 0.77 (t, J = 7 Hz, 3H). ^{13}C NMR (75 MHz, $CDCl_3$) δ 182.6, 166.6, 163.7, 159.6, 157.3, 131.7, 129.2, 126.4, 107.9, 105.6, 95.1, 77.7, 77.2, 76.8, 58.3, 35.1, 34.3, 31.9, 25.6, 22.7, 14.2. HRMS: m/z $[M + H]^+$ calcd for $C_{22}H_{26}NO_4$, 368.1862; found, 368.1869. Enantiomeric separation of (±)-**18** by chiral HPLC: 400 mg of F1 was next subjected to SFC HPLC separation using column IC, 20% cosolvents (MeOH/diethylamine 98:2), flow rate 4 mL/min; t_{R1} = 9.7 min, 165 mg, *ee* = 96%, $[\alpha]_D^{23}$ +62.3 (*c*, 0.12, $CHCl_3$), configuration *R*; t_{R2} = 13.3 min, 159 mg, *ee* = 99%, $[\alpha]_D^{23}$ −65.4 (*c*, 0.26, $CHCl_3$), configuration *S* (determined by X-ray diffraction).

5.3. Molecular Modeling. Crystal structures were downloaded from the Protein Data Bank (PDB), and residues not belonging to the protein were removed, including water molecules. The homology model of CDK1 was built with MODELER[26] v9.7 using the X-ray structure of CDK2 (PDB code 1YKR) and the sequence alignment shown in Figure S2 of the Supporting Information), generated using the ClustalW[27] software (v1.8). Several homology models (100) were built, and the one with the best DOPE energy score retained for the molecular docking step. For both PDB structures and homology models, the hydrogen atoms were added and energy minimized with OPLS2005 force field (standard parameters from Schrödinger's Protein Preparation Wizard Workflow), keeping all heavy atoms fixed.

Three-dimensional structures of ligands were generated using CORINA[28] v3.44, and then all combinations of stereoisomers and protonation states at pH 7.0 ± 2.0 were calculated with the LigPrep module from the Schrodinger Suite.[29] Whenever the absolute configuration of a chiral center in the ligand structure was unknown, both isomers were considered in the docking process. The amino groups at C-8 in all flavonoidal compounds were used in the protonated form throughout this work.

Molecular docking calculations were performed using GOLD 5.0 software[30] with both GoldScore and Chemscore_Kinase scoring functions. After 200 genetic algorithm (GA) runs with 100000 GA operations per docking, clusters were created at 2.0 Å rmsd. Ligand flexibility was allowed to explore ring conformations and flip ring corners. After docking, the complex was minimized using Schrödinger's Maestro framework[31] taking into account protein residues within 8.0 Å from the ligand. Visual inspection of the resulting clusters showed that in most cases the lowest energy cluster presented the correct positioning in the binding site, with a conformation similar to the one adopted by flavopiridol in the CDK9 crystal structure (see Figure S3, Supporting Information). In the other few instances, this correct positioning related to flavopiridol was found in the second cluster (and once in the third cluster). In these latter cases, the differences between the score of the selected complex and the score of the lowest energy complex were not significant (less than 10%).

Images of the protein−ligand complexes were rendered using PyMol version 0.99.[32]

■ ASSOCIATED CONTENT

Supporting Information

Experimental details, NMR, mass, HPLC chromatograms of racemic and enantiomers data, X-ray data, X-ray structures of (−)-**1**, (+)-**15**, and (−)-**18**, table with residue variability in the binding sites of kinases and sequence alignment used for homology modeling. This material is available free of charge via the Internet at http://pubs.acs.org.

■ AUTHOR INFORMATION

Corresponding Author

*For chemistry (F.G.): phone, +33 (0) 1 69 82 45 80; E-mail, gueritte@icsn.cnrs-gif.fr. For biology (L. M.): phone, +33 (0) 2 98 29 23 39; E-mail, meijer@manros-therapeutics.com.

Notes

The authors declare no competing financial interest.

■ ACKNOWLEDGMENTS

Kinase assays were supported by grants from "Association France-Alzheimer" (Comité du Finistère) (L.M.), INCa (Institut National du Cancer) "Recherches Biomédicales" (GLIOMER project) (L.M.), "Fonds Unique Interministeriel" (PHARMASEA project) (L.M.), and "Ligue Nationale contre le Cancer" (Comité du Finistère) (L.M.).

■ ABBREVIATIONS USED

CDK, cyclin-dependent kinase; GSK3, glycogen synthase kinase-3; DYRK1A, dual specificity tyrosine-phosphorylation-regulated kinase 1A; CLK1, CDC-like kinase 1; ATP, adenosine 5′-triphosphate; SFC, supercritical fluid chromatography; HPLC, high-performance liquid chromatography; THF, tetrahydrofuran; $[\alpha]$, specific rotation; μM, micromolar; IC_{50}, half-maximum inhibitory concentration; PDB, Protein Data Bank; rmsd, root-mean-square deviation; Val, valine; Ala,

alanine; Leu, leucine; Cys, cysteine; Asp, aspartic acid; Asn, asparagine; Lys, lysine; Gln, glutamine; Arg, arginine; Tyr, tyrosine; Thr, threonine; Phe, phenylalanine; mM, millimolar; EGTA, ethylene glycol tetraacetic acid; DTT, dithiothreitol; BSA, bovine serum albumin; DMSO, dimethyl sulfoxide; GST, glutathione S-transferase; TLC, thin layer chromatography; UV, ultraviolet; TMS, tetramethylsilane; s, singlet; d, doublet; t, triplet; q, quartet; m, multiplet; ESI, electron spray ionization; AcOEt, ethyl acetate; MeOH, methanol; NMR, nuclear magnetic resonance; HRMS, high resolution mass spectrometry; iPrOH, isopropanol; ee, enantiomeric excess; rt, room temperature; tr, retention time; $MeNH_2$, methylamine; DOPE, discrete optimized protein energy; GA, genetic algorithm

REFERENCES

(1) Diaz-Padilla, I.; Siu, L. L.; Duran, I. Cyclin-dependent kinase inhibitors as potential targeted anticancer agents. *Invest. New Drugs* **2009**, *27*, 586−594.

(2) Meijer, L.; Flajolet, M.; Greengard, P. Pharmacological inhibitors of glycogen synthase kinase 3. *Trends Pharmacol. Sci.* **2004**, *25*, 471−480.

(3) Park, J.; Song, W.-J.; Chung, K. C. Function and regulation of Dyrk1A: towards understanding Down syndrome. *Cell. Mol. Life Sci.* **2009**, *66*, 3235−3240.

(4) Moeslein, F. M.; Myers, M. P.; Landreth, G. E. The CLK family kinases, CLK1 and CLK2, phosphorylate and activate the tyrosine phosphatase, PTP-1B. *J. Biol. Chem.* **1999**, *274*, 26697−26704.

(5) Ahond, A.; Fournet, A.; Moretti, C.; Philogene, E.; Poupat, C.; Thoison, O.; Potier, P. Premiers Alcaloides vrais isolés de Combrétacées, *Buchenavia macrophylla* Eichl. et *Buchenavia capitata* Eichl. *Bull. Soc. Chim. Fr.* **1984**, *1*−*2* (Pt2), 41−45.

(6) Beutler, J. A.; Cardellina, J. H. II; McMahon, J. B.; Boyd, M. R. Anti-HIV and cytotoxic alkaloids from *Buchenavia capitata*. *J. Nat. Prod.* **1992**, *55*, 207−213.

(7) Khoo, B. Y.; Chua, S. L.; Balaram, P. Apoptotic Effects of Chrysin in Human Cancer Cell Lines. *Int. J. Mol. Sci.* **2010**, *11*, 2188−2199.

(8) Senderowicz, A. M. Flavopiridol: the first cyclin-dependent kinase inhibitor in human clinical trials. *Invest. New Drugs* **1999**, *17*, 313−320.

(9) Raje, N.; Hideshima, T.; Mukherjee, S.; Raab, M.; Vallet, S.; Chhetri, S.; Cirstea, D.; Pozzi, S.; Mitsiades, C.; Rooney, M.; Kiziltepe, T.; Podar, K.; Okawa, Y.; Ikeda, H.; Carrasco, R.; Richardson, P. G.; Chauhan, D.; Munshi, N. C.; Sharma, S.; Parikh, H.; Chabner, B.; Scadden, D.; Anderson, K. C. Preclinical activity of P276−00, a novel smallmolecule cyclin-dependent kinase inhibitor in the therapy of multiple myeloma. *Leukemia* **2009**, *23*, 961−970.

(10) Liu, T.; Xu, Z.; He, Q.; Chen, Y.; Yang, B.; Hu, Y. Nitrogen-containing flavonoids as CDK1/cyclin B inhibitors: design, synthesis, and biological evaluation. *Bioorg. Med. Chem. Lett.* **2007**, *17*, 278−281.

(11) Zhang, S.; Ma, J.; Bao, Y.; Yang, P.; Zou, L.; Li, K.; Sun, X. Nitrogen-containing flavonoid analogues as CDK1/cyclin B inhibitors: synthesis, SAR analysis, and biological activity. *Bioorg. Med. Chem.* **2008**, *16*, 7127−7132.

(12) Johns, S. R.; Russel, J. H.; Hefferman, M. L. Ficine, A novel flavonoidal alkaloid from *Ficus pantoniana*. *Tetrahedron Lett.* **1965**, *24*, 1987−1991.

(13) Leete, E. One-Step Synthesis of Ficine and Isoficine. *J. Nat. Prod.* **1982**, *45*, 605−607.

(14) Nguyen, T.-B.; Wang, Q.; Guéritte, F. An efficient one-step synthesis of piperidin-2-yl and pyrrolidin-2-yl flavonoidal alkaloids through phenolic Mannich reaction of flavonoid and cyclic imines. *Eur. J. Org. Chem.* **2011**, 7076−7079.

(15) Wessely, F.; Moser, G. H. Synthese und Konstitution des Skutellareins. *Monatsh. Chem.* **1930**, *56*, 97−105.

(16) Shinomiya, K.; Hano, Y.; Nomura, T. Mechanism on one-sided Wessely−Moser Rearrangement Reaction. *Heterocycles* **2000**, *53*, 877−886.

(17) Berman, H. M.; Battistuz, T.; Bhat, T. N.; Bluhm, W. F.; Bourne, P. E.; Burkhardt, K.; Feng, Z.; Gilliland, G. L.; Iype, L.; Jain, S.; Fagan, P.; Marvin, J.; Padilla, D.; Ravichandran, V.; Schneider, B.; Thanki, N.; Weissig, H.; Westbrook, J. D.; Zardecki, C. The Protein Data Bank. *Acta Crystallogr., Sect. D: Biol. Crystallogr.* **2002**, *58*, 899−907.

(18) Mapelli, M.; Massimiliano, L.; Crovace, C.; Seeliger, M. A.; Tsai, L. H.; Meijer, L.; Musacchio, A. Mechanism of CDK5/p25 binding by CDK inhibitors. *J. Med. Chem.* **2005**, *48*, 671−679.

(19) Aoki, M.; Yokota, T.; Sugiura, I.; Sasaki, C.; Hasegawa, T.; Okumura, C.; Ishiguro, K.; Kohno, T.; Sugio, S.; Matsuzaki, T. Structural insight into nucleotide recognition in tau-protein kinase I/glycogen synthase kinase 3 beta. *Acta Crystallogr., Sect. D: Biol. Crystallogr.* **2004**, *60*, 439−446.

(20) Hamdouchi, C.; Zhong, B.; Mendoza, J.; Collins, E.; Jaramillo, C.; De Diego, J. E.; Robertson, D.; Spencer, C. D.; Anderson, B. D.; Watkins, S. A.; Zhang, F.; Brooks, H. B. Structure-based design of a new class of highly selective aminoimidazo[1,2-*a*]pyridine-based inhibitors of cyclin dependent kinases. *Bioorg. Med. Chem. Lett.* **2005**, *15*, 1943−1947.

(21) Baumli, S.; Lolli, G.; Lowe, E. D.; Troiani, S.; Rusconi, L.; Bullock, A. N.; Debreczeni, J. E.; Knapp, S.; Johnson, L. N. The structure of P-TEFb (CDK9/cyclin T1), its complex with flavopiridol and regulation by phosphorylation. *EMBO J.* **2008**, *27*, 1907−1918.

(22) Bettayeb, K.; Oumata, N.; Echalier, A.; Ferandin, Y.; Endicott, J. A.; Galons, H.; Meijer, L. CR8, a potent and selective, roscovitine-derived inhibitor of cyclin-dependent kinases. *Oncogene* **2008**, *27*, 5797−5807.

(23) Primot, A.; Baratte, B.; Gompel, M.; Borgne, A.; Liabeuf, S.; Romette, J. L.; Costantini, F.; Meijer, L. Purification of GSK-3 by affinity chromatography on immobilised axin. *Protein Expression Purif.* **2000**, *20*, 394−404.

(24) Gravel, E.; Poupon, E.; Hocquemiller, R. Biomimetic investigations from reactive lysine-derived C_5 units: one step synthesis of complex polycyclic alkaloids from the *Nitraria* genus. *Tetrahedron* **2006**, *62*, 5248.

(25) Nomura, Y.; Ogawa, K.; Takeuchi, Y.; Tomoda, S. One-Step Synthesis and Structural Confirmation of 1-Pyrroline Trimer. *Chem. Lett.* **1977**, *6*, 693.

(26) Šali, A.; Potterton, L.; Yuan, F.; van Vlijmen, H.; Karplus, M. Evaluation of comparative protein modeling by MODELLER. *Proteins: Struct., Funct., Bioinf.* **1995**, *23*, 318−326.

(27) Thompson, J. D.; Higgins, D. G.; Gibson, T. J. CLUSTAL W: improving the sensitivity of progressive multiple sequence alignment through sequence weighting, position-specific gap penalties and weight matrix choice. *Nucleic Acids Res.* **1994**, *22*, 4673−4680.

(28) *CORINA, version 3.44*; Molecular Networks GmbH: Erlangen, Germany, 2008; http://www.molecular-networks.com (Accessed December 15, 2011).

(29) *LigPrep, version 2.5*; Schrödinger, LLC: New York, 2011; http://www.schrodinger.com (Accessed December 15, 2011).

(30) Verdonk, M. L.; Cole, J. C.; Hartshorn, M. J.; Murray, C. W.; Taylor, R. D. Improved protein−ligand docking using GOLD. *Proteins: Struct., Funct., Bioinf.* **2003**, *52*, 609−623.

(31) *Maestro, version 9.2*; Schrödinger, LLC: New York, 2011; http://www.schrodinger.com (Accessed December 15, 2011).

(32) *The PyMOL Molecular Graphics System, version 0.99*; DeLano Scientific: Palo Alto, CA, 2006; http://www.pymol.org (Accessed December 15, 2011).